CHAPTER IV
A NOVEL ROOM TEMPERATURE SYNTHESIS OF MESOPOROUS SBA-15 FROM SILATRANE

4.1 Abstract

Well-ordered and stable two dimensional mesoporous silica, SBA-15, were synthesized at room temperature (RT) from a silatrane precursor and a non-ionic triblock copolymer ($EO_{20}PO_{70}EO_{20}$) as the structure directing agent. Using a combination of small angle X-ray scattering, electron microscopy and nitrogen gas absorption-desorption isotherms, the RT product was found to be equivalent to SBA-15 prepared using more elaborative microwave-assisted hydrothermal methods. Both synthesis routes yielded large surface areas (486–613 m^2/g), pore diameters (45–67 Å) and channel volumes (0.6–0.8 cm^3/g). All materials condensed as sinuous bundles of silica tubes, in a morphology that approximates *p6mm* symmetry, but where long range order was absent. In addition, a portion of the products consisted of fine crystalline mosaics or were aperiodic. The simplicity of the room temperature synthesis route may provide an inexpensive and energy-saving process for the large scale production of thermally stable SBA-15 as a catalyst support.

(**Keywords**: Silatrane, SBA-15, Synthesis, non-ionic triblock copolymer)

4.2 Introduction

Mesoporous materials have been of wide scientific and technological interest since the discovery of the M41S family in the 1990s by the Mobil research group [1, 2]. Among the mesoporous silicas, the SBA group has attracted attention by virtue of their thicker walls, greater hydrothermal stability and larger pore size as compared to the M41S materials. In particular, well-ordered hexagonal SBA-15 possesses high specific surface areas (characteristically 600–1000 m^2/g), large pore sizes (45–300 Å) and excellent hydrothermal stability (up to 850 °C). These superb properties, place SBA-15 in demand for catalytic, adsorption and separation

applications that require high temperature or operate in corrosive environments [3-10]. Mesoporous silicas are typically synthesized by sol-gel processes where structure-directing amphiphillic surfactants, such as poly(ethylene glycol)-block-poly(propylene glycol)-block-poly(ethylene glycol), self assemble as micelles which are encapsulated by an inorganic silica precursor [11]. Calcination at 500–600 °C oxidizes the surfactant, leaving thee- or two-dimensional mesoporous arrangements of cavities or channels [12-16].

SBA-15 is a 2D mesoporous material first prepared hydrothermally under acidic conditions (pH 1-2) using tetraethyl orthosilicate (TEOS) as the silica source and triblock copolymers to direct the organization of the polymerizing silica species [6-7]. Generally, a hydrothermal treatment time of 11–72 h at 100 °C was needed to yield well-ordered mesoporous structures of high surface area (690 m^2/g), uniform pore diameter (47 Å) and volume (0.56 cm^3/g). Subsequently, Newalkar *et al.* [17] introduced microwave-assisted syntheses to shorten reaction time (2 h) while obtaining materials of similar quality to those prepared in the autoclave. The microwave method proves superior as volumetric heating favors homogeneous nucleation, and fast dissolution and supersaturation of precipitated gels promotes shorter crystallization times [18-30].

Previous work has shown that controlling hydrolysis and condensation is key to preparing well-ordered mesoporous material though sol-gel processing [31]. While TEOS is a common silica source, it is highly susceptible to hydrolysis, and the rapid separation of amorphous silica impedes mesopore formation. Therefore, it is advantageous to use precursors of reduced hydrolytic activity such as silatrane, an organosilicate resistant towards hydrolysis that is stable in air for several weeks. Additionally, silatrane is an inexpensive silica precursor, which can be conveniently synthesized directly from fumed silicon dioxide and triethanolamine in ethylene glycol [32-33]. These starting materials are commercially available and low-priced. Silatrane is a proven silica precursor for the sol-gel synthesis of many microporous [34-37] and mesoporous [38-42] zeolites. In this paper, we describe a simple room temperature route for the preparation of SBA-15 using silatrane under acidic conditions, where a triblock copolymer (pluronic P123) was employed as the

structure-directing agent. The demonstration of room temperature synthesis shows that large scale production of SBA-15 can be economical and energy efficient.

4.3 Experimental section

4.3.1 Silatrane Synthesis

The silatrane precursor was synthesized from fumed silica (99.8%, Sigma-Aldrich, St. Louis, MO) solubilized in triethanolamine (TEA) (Carlo Erba, Milan, Italy), with ethylene glycol (EG) (J.T. Baker, Philipsburg, NJ) employed as the solvent, and acetronitrile (Labscan, Bangkok, Thailand) used for silatrane purification. Following the method of Wongkasemjit *et al.* [43], 0.125 mol TEA was refluxed with 0.1 mol silicon dioxide in ethylene glycol (100 ml) at 200 °C under nitrogen for 10 h in an oil bath. Excess ethylene glycol was removed under vacuum at 110 °C to obtain a crude brown solid that was washed with acetronitrile to remove TEA and EG residues. The white silatrane product was vacuum dried overnight then examined by Fourier-transform infrared (FT-IR) absorption spectrometery (Bruker Optics EQUINOX55, Karlsruhe, Germany) at a resolution of 2 cm^{-1}, and thermogravimetric analysis (DuPont 2950, Twin Lakes, WI) at a heating rate of 10 ^{o}C/min from room temperature to 750 °C in a nitrogen atmosphere.

The FT-IR bands observed were 3000–3700 cm^{-1} (w, νO–H), 2860–2986 cm^{-1} (s, νC–H), 1244–1275 cm^{-1} (m, νC–N), 1170–1117 cm^{-1} (bs, νSi–O), 1093 cm^{-1} (s, νSi–O–C), 1073 cm^{-1} (s, νC–O), 1049 cm^{-1} (s, νSi–O), 1021 cm^{-1} (s, νC–O), 785 and 729 cm^{-1} (s, νSi–O–C), and 579 cm^{-1} (w, νN-Si). TGA showed one sharp mass loss at 390 °C and gave a 19% ceramic yield of $N(CH_2CH_2O)_3Si–OCH_2CH_2–N(CH_2CH_2OH)_2$.

4.3.2 SBA-15 Synthesis

Mesoporous SBA-15 was synthesized from silatrane with poly(ethylene glycol)-block-poly(propylene glycol)-block-poly(ethylene glycol) ($EO_{20}PO_{70}EO_{20}$) (P123) (Sigma-Aldrich) employed as the template, and hydrochloric acid (Labscan Asia) as the catalyst in accord with the procedure of Stucky *et al.* [6-7]. A solution of $EO_{20}PO_{70}EO_{20}$:HCl:silatrane:H_2O = 2:60:4.25:12 (mass ratio) was

prepared by dissolving 4 g of $EO_{20}PO_{70}EO_{20}$ polymer in 80 g of 2 M HCl (part A) and 8.8 g of silatrane in 20 g of H_2O (part B) with stirring continued for 1 h to ensure complete dissolution. For Route 1 synthesis, the solution of part B was then poured into part A, stirred at room temperature (RT) for 24 h, the product was recovered by filtration, washed with deionized water, and dried overnight under ambient conditions. For Route 2, the RT product was in addition treated in an autoclave placed in a microwave oven at 300W for 1–2 h at 100 or 120 °C. After cooling to RT, the material was filtered, washed and dried as for the Route 1 SBA-15. Both Route 1 and Route 2 silicas were calcined at 550 °C in air for 6 h using a tube furnace (Carbolite, CFS 1200, Hope Valley, U.K.) at a heating rate of 1 °C/min to remove the residual organics (Figure 1). The microwave assisted product prepared at 120 °C was taken as the baseline material.

4.3.3 Characterization

Mesopore Ordering: Small-angle X-ray scattering (SAXS) patterns were obtained with a PANalytical PW3830 X-ray instrument using CuKα radiation generated at 50kV and 40 mA. Thin powder samples (0.02 g) were spread uniformly on adhesive tape and mounted on an aluminium frame (15–20 mm). The scattering patterns were recorded on an image plate and intensities extracted as two dimensional plots against scattering angle (2θ) by integration across approximately 450 pixels/degree 2 theta (Figure 2a). As replication of the 2θ zero shift was poor, the relative, rather than absolute positions of the scattering maximum were compared. By using identical sample weights the intensity of the peaks could be directly compared. If the stacking of silica mesotubes is perfectly hexagonal and conforms to *p6mm* plane symmetry than the 2D crystallographic repeat can be indexed as {10} ≡ {11}, while the second order reflections provide a measure of the channel diameter and can be indexed as {30} ≡ {33} (Figure 2b). Additional scattering (e.g. {-1-1} or {-2-1}) out to larger d-spacings will be significant only if the coherent hexagonal domain sizes are sufficiently extensive.

Nanostructure: Field Emission Scanning Electron Microscope (FESEM) images were obtained from powders mounted on double-sided carbon tape using a JEOL JSM-7500F, operating at an accelerating voltage of 0.3–0.5 kV to

minimize the effects of charging. Transmission electron microscopy (TEM) was conducted using a JEOL JEM-2100F TEM instrument operated at an accelerating voltage of 200 kV with a large objective aperture. For TEM, the powder was lightly ground under ethanol, sometimes with the introduction of liquid N_2 to enhance fracture and produce thin flakes that were dispersed ultrasonically. Two drops of the suspension were deposited on holey carbon-coated copper grids. The periodicity of SBA-15 projected along the mesotubes were studied by fast Fourier transformation of TEM images using CRISP [44] to extract interplanar angles, with deviations from 60° indicating an oblique rather than hexagonal metric. The average size of the channels was obtained by assuming *p6mm* symmetry and carrying out a back Fourier transform with the diameter measured directly from the reprocessed image.

Physical Parameters: Nitrogen sorption isotherms were obtained at -196 °C after out gassing at 250 °C for 12 h (Quantasorb JR, Mount Holly, NJ). The surface area and average pore size were determined by the Brunauer–Emmett–Teller (BET) method.

4.4 Results and Discussion

4.4.1 As-synthesized SBA-15 mesoporous material

The SAXS pattern for as-synthesized mesoporous silica (SBA-15) prepared with $EO_{20}PO_{70}EO_{20}$ shows two well-resolved peaks (Figure 2A) that are indexable as {10} ≡ {11} and {30} ≡ {33} reflections associated with *p6mm* hexagonal symmetry. The intense {10} peak reflects a *d* spacing of 150 Å, corresponding to a unit-cell parameter (a_0 = 173 Å). After calcination in air at 550 °C for 6 h, SAXS (Figure 2B) shows that the *p6mm* morphology is preserved. Two peaks are still observed, confirming that hexagonal SBA- 15 is thermally stable. A similarly high degree of mesoscopic order is observed for hexagonal SBA-15 even after calcination at 850 °C.

Thermal gravimetric and differential thermal analyses (TGA and DTA) in air of the SBA-15 sample calcined at 550 °C for 6 h and prepared with $EO_{20}PO_{70}EO_{20}$ show total weight losses of 11.02 weight % (Figure 3). At 94.6 °C,

TGA registers a 2.11 weight % loss because of desorption of water. There is no weight loss at 145 °C which would correspond to the decomposition temperature of the block copolymer[6] indicating that there is no any nitrogen or carbon species left in the mesoporous wall, and confirming that the template has completely been removed.

4.4.2 With hydrothermal treatment

A. High temperature microwave-assisted hydrothermal synthesis (120 °C/1 h): This benchmark material yielded a SAXS pattern with first and second order scattering centered at d-spacings of 182.5 Å (a_o = 210.7 Å) and 65.8 Å (Figure 5a). When indexed according to the plane group *p6mm* as {10} ≡ {11} and {30} ≡ {33}, the ratio $d_{\{10\} \equiv \{11\}} / d_{\{30\} \equiv \{33\}} = 2.8$, rather than 3, since the overall structure shows significant deviations from the hexagonal metric, and more nearly conforms to oblique *p*2 (Table 1). Both scattering maxima are anisotropic such that {10} ≡ {11} shows a sharp upper limit of the d-spacing at ~190 Å, but a long tail towards higher scattering angles down to ~167 Å (Figure 5b), while the {30} ≡ {33} feature is asymmetric in an opposite sense and spans channel diameters from 63–67 Å. Higher order features such as {-1-1} are barely discernable because the coherent hexagonal domains were quite restricted (Figure 5b). Microscopy confirmed the absence of longer range periodicity as implied by SAXS. Field Emission scanning electron microscope (FESEM) showed that SBA-15 possesses a sinuous morphology at the scale of a few hundred nanometers and coexisted with poorly ordered mesopore fragments (Figure 6a). In TEM, the mosaic character of even the better ordered fragments was evident (Figue 6b). At higher magnifications FESEM suggests that the channels are partially cavitated, rather than open conduits, which would limit mass transport (Figure 6c), however the TEM images show the projected absorption contrast and periodicity are insensitive to random channel blockages (Figure 6d). In detail, images collected parallel to the pseudo 6-fold rotation axis clearly show variability in both channel diameter and filling (Figure 6e), while <10> ≡ <11> projections confirm tubule ordering (Figure 6f).

Fast Fourier transform analysis of 6-fold TEM projections confirmed that departures from *p6mm* symmetry were systemic, with the {10} ≡ {11} interplanar angles deviating from 60° (Figure 7a,b). By imposing hexagonal

symmetry as the average structure and applying the back Fourier reconstruction, a processed image is recovered from which the pore diameter is directly accessible (Figure 7a) and shows an average tunnel diameter of 46 Å. The pore diameters derived from SAXS and TEM image processing, bracket the value obtained by nitrogen adsorption measurements, which gave a diameter of 54 Å (Table 1), pore volume of 0.8 cm^3/g and a high surface area (613 m^2/g) (Figure 8a). The isotherm was an IUPAC type IV with an H1-type hysteresis loop [5]. However, SBA-15 synthesized from silatrane showed a smaller pore volume (0.8 cm^3/g) and surface area (613 m^2/g) compared to equivalent material synthesized from TEOS (0.99 cm^3/g and 805.9 m^2/g). This is consistent with the SAXS observation that the silatrane source yielded less well-ordered mesopores [6, 7, 16]. While the TEOS derived SBA-15, X-ray scattering patterns contain up to four peaks indicative of longer range periodicity.

B. Low temperature microwave-assisted hydrothermal synthesis (100 ℃/2h): The characteristics of SBA-15 prepared at 100 °C were broadly similar to those of the 120°C material, with the $d_{\{10\} \equiv \{11\}} / d_{\{30\} \equiv \{33\}} = 2.8$ (Figure 5) and a cavitated channel structure (Figure 9). The surface area (572 m^2/g) and pore diameter (55 Å) are identical to those obtained at 120 °C / 1 h (Figure 8b).

Generally, the work related to SBA-15 employs a hydrothermal treatment step via autoclave or microwave assisted methods using TEOS as a silica source, and P123 as the template. For example, Su *et al.* [45], studied the orientation of mesochannels using a laser-modified polyimide surface, with TEOS was employed as silica source and P123 as the structure directing agent. The material was hydrothermally treated in an autoclave at 110 °C for 48 h. The orientation of the mesochannels was evaluated by X-ray scattering measurement. One narrow {10} peak of the 2D hexagonal phase appeared. The absence of a {11} peak, which would normally be observed in a hexagonal structure, was consistent with the mesopore channels oriented parallel to the substrate. Okamoto *et al.* [46], studied the site-specific synthesis of mixed valence Ti-O-Fe complexes within the pores of ordered mesoporous silica SBA-15 using TEOS and P123. The powder exhibited thee reflections corresponding to {10}, {11} and {20} of a two-dimensional hexagonal

pore structure. Newalkar *et al.* [17] reported a microwave-assisted synthesis method to shorten the synthesis time that employed TEOS and P123, that can be reduced the reaction time to 2 h and yield the product similar to that prepared by 48 h conventional autoclave treatment. It is believed the rapid heating to the crystallization temperature by volumetric heating favored homogeneous nucleation, fast supersaturation by the rapid dissolution of precipitated gels, and ultimately a shorter crystallization time.

Zhao *et al.* [6-7], used TEOS and P123 to synthesize SBA-15 in acidic conditions as a function of temperature and time. Using an autoclave, it took 48 h to complete the reaction and achieve well-ordered SBA-15 with high surface area (690 m^2/g), uniform pore size of (47 Å) and pore volume (0.56 cm^3/g), these results are similar to the data obtained from the sample from this work.

4.4.3 Without hydrothermal treatment

Direct RT synthesis : The relative positions of the SAXS scattering maxima appear at 182.5 Å and 60.8 Å and conform almost exactly to the hexagonal metric with $d_{\{10\} \equiv \{11\}} / d_{\{30\} \equiv \{33\}} = 3.0$ (Figure 5). The spread of crystallographic repetition is unchanged (190 – 167 Å), however the channel diameter is slightly smaller (63 – 60 Å), in agreement with the BET measurements that yielded a surface area (486 m^2/g) and pore diameter (50 Å) (Figure 8c), Table 1). Micrograph collected near the principal axial projections are indistinguishable from the hydrothermally prepared material (Figure 10).

SAXS indicates that SBA-15 prepared at RT are well-ordered 2D mesoporous materials, comparable to those microwave-assisted hydrothermal products, with the latter yielding a marginally superior product in terms of higher BET surface area and mesopore order. When conventional precursors such as TEOS are used, it is believed that the hydrothermal conditions promote the condensation of metal oxide bridges, leading to better ordered structures. However, this benefit is minimal when silatrane is employed, as it is stable towards hydrolysis and can be employed at room temperature. Tanglumlert *et al.* [48] reported the successful synthesis of well-ordered and stable SBA-1 mesoporous silica via sol-gel process using silatrane as a silica source. The high quality SBA-1 was produced under mild

acidic condition, C_nTMAB was used as a template, and the reaction was conducted at room temperature.

As it can be seen from the TEM images, the silica wall thickness between RT and microwave-assisted hydrothermal samples are equally similar, implying that silatrane condensation of Si-O-Si takes place at room temperature. By operating at ambient, this method minimizes process complexity while forming well-ordered SBA-15. The results from SAXS, FESEM and TEM clearly indicate that SBA-15 obtained from the room temperature (without hydrothermal treatment), and microwave-assisted method are comparable, and would facilitate economical and energy saving large scale production.

4.5 Conclusions

It has been demonstrated that SBA-15 can be successfully synthesized at room temperature using silatrane, an inexpensive and conveniently prepared silica, as the silica precursor. The crystallographic, morphological and physical properties of SBA-15 obtained by this simple process are comparable to mesoporous silica prepared by the more complex microwave-assisted hydrothermal method. This new preparative route may allow inexpensive, energy-saving and efficient production of SBA-15 for a range of catalytic and environmental applications.

4.6 Acknowledgements

This research work is financially supported by the Postgraduate Education and Research Program in Petroleum and Petrochemical Technology (ADB) Fund (Thailand), the Ratchadapisake Sompote Fund, Chulalongkorn University, and the Thailand Research Fund (TRF). We thank Mr Tan Teck Siong for assistance in collecting the secondary electron images, and the School of Materials Science & Engineering NTU for partially financial support.

4.7 References

1. Kresge, C. T.; Leonowicz, M. E.; Roth, W. J.; Vartuli, J. C.; Beck, J. S. *Nature* 1992, *359*, 710-712.
2. Beck, J. S.; Vartuli, J. C.; Roth, W. J.; Leonowicz, M. E.; Kresge, C. T.; Schmitt, K. D.; Chu, C. T. W.; Olson, D. H.; Sheppard, E. W.; McCullen, S. B.; Higgins, J. B.; Schlenker, J. L. *J. Am. Chem. Soc.* 1992, *114*, 10834-10843.
3. Davis M. E. *Chem. Ind.* 1992, *4*, 137.
4. Estermann M.; McCusker L. B.; Baerlocher C.; Merroche A.; Kessler H. *Nature* 1991, *352*, 320.
5. Hoang V-T.; Huang Q.; Ei M.; Do T-O.;Kaliaguine S. *Langmuir* 2005, *21*, 2051-2057
6. Zhao, D.; Feng, J.; Huo, Q.; Melosh, N.; Frerickson, G. H.; Chmelka, B. F.; Stucky, G. D. *Science* 1998, *279*, 548-552.
7. Zhao, D.; Huo, Q.; Feng, J.; Chmelka, B. F.; Stucky, G. D. *J. Am. Chem. Soc.* 1998, *120*, 6024-6036.
8. Trong-On, D.; Desplantier-Giscard, D.; Danumah, D.; Kaliaguine, S. *Appl. Catal.*, A 2001, *222*, 299-357.
9. Kubo S.; Kosuge K.; *Langmuir*, 2007, *23*, 11761-11768.
10. Coasne B.; Galarneau A.; Renzo D.F.; Pellenq R.J.M. *Langmuir* 2006, *22,* 11097-11105.
11. Kruk M.; Cao L. *Langmuir* 2007, *23,* 7247-7254.
12. Goltner C. G.; Antonietti M. *Adv Mater.* 1997, *9*, 431.
13. Antonietti M.; Goltner C. *Angew. Chem. Int. Ed. Engl.* 1997, *36*, 910.
14. Wanka G.; Hoffmann H.; Ulbricht W. *Macromolecules* 1994, *27*, 4145.
15. Chu B.; Zhou, *Surfactant Science Series* 1996, *60*, 67.
16. Zukal A.; Siklova H.; Cejka J. L*angmuir* 2008, *24,* 9837-9842.
17. Newalkar B.; Komarneni S.; Katsuki H. *Chem. Commun.* 2000, 2389-2390.
18. Komarneni S.; Roy R.; Li Q. H. *Mater. Res. Bull.* 1992, *27*, 1393.
19. Komarneni S.; Li Q. H.; Stefansson K. M.; Roy R. *J. Mater. Res.* 1993, *8*, 3176.
20. Komarneni S.; Li Q. H.; Roy R. *J. Mater. Chem.* 1994, *4*, 1903.
21. Komarneni S.; Pidugu R.; Li Q. H.; Roy R. *J. Mater.Res.* 1995, *10*, 1687.
22. Komarneni S.; Li Q. H.; Roy R. *J. Mater. Res.*1996, *11*, 1866.
23. Komarneni S.;. Menon V. C. *Mater. Lett.* 1996, *27*, 313.

24. Chu P.; Dwyer F. G.; Vartuli J. C. *US Pat.* 1988, 4 778 666.
25. Lohe U.; Bertram R.; Jancke K.; Kurzawski I.; Parlitz B.; Loeffler E.; Scheier E. *J. Chem. Soc., Faraday Trans.* 1995, *91*, 1163.
26. Girnus I.; Jancke K.; Vetter R.; Richter-Mendau J.; Caro J. *Zeolites* 1995, *15*, 33.
27. Meng X.; Xu W.; Tang S.; Pang W. *Chin. Chem. Lett.* 1992, *3*, 69.
28. A. Arafat, J. C. Jansen, A. R. Ebaid and H. Van Bekkum, *Zeolites*, 1993, *13*, 162.
29. Wu C. G.; Bein T. *Chem. Commun.* 1996, 925.
30. Park M.; Komarneni S. *Microporous Mesoporous Mater.*, 1998, *20*, 39.
31. Cabrera S.; Haskouri J. E,; Guillem C.; Latorre J.; Beltran-porter A.; Beltran-porter D.; Marcos M. D.; Amoros P.; *Solid state Sci* 2000, *2*, 405.
32. Phiriyawirut P.; Magaraphan R.; Jamieson A. M.; Wongkasemjit S. *Material Science and Engineering* 2003, *A361*, 147-154.
33. Charoenpinijkarn W.; Suwankruhasn M.; Kesapabutr B.; Wongkasemjit S.; Jamieson A. M. *European Polymer Journal* 2001, *37*, 1441-1448.
34. Sathupanya M.; Gulari E.; Wongkasemjit S. *J. Eur. Ceram. Soc.* 2002, *22*, 1293–1303.
35. Sathupanya M.; Gulari E.; Wongkasemjit S. *J. Eur. Ceram. Soc.* 2003, *23*, 2305–2314.
36. Phonthammachai N.; Chairassameewong T.; Gulari E.; Jameison A. M.; Wongkasemjit S. *J. Met. Mater. Min.* 2003, *12*, 23.
37. Phiriyawirut P.; Jamieson A. M.; Wongkasemjit S. *Microporous Mesoporous Mater.* 2005, *77*, 203–213.
38. Thanabodeekij N.; Tanglumlert W.; Gulari E.; Wongkasemjit S. *Appl. Organomet. Chem.* 2005, *19*, 1047–1054.
39. Thanabodeekij N.; Sadthayanon S.; Gulari E.; Wongkasemjit S. *Mater. Chem. Phys.* 2006, *98*, 131–137.
40. S. Mintova J. Cejka, *Stud. Surf. Sci. Catal.* 2007, *168*, 301-326
41. J. Cejka, S. Mintova, *Catal. Rev.* 2007, *49*, 457-509
42. Perez-Ramirez J, Chistensen CH, Egeblad K, Chistensen CH, Groen JC, *Chem. Soc. Rev.* 2008, *37*, 2530-2542
43. Piboonchaisit P.; Wongkasemjit S.; Laine R. *J. Sci. Soc. Thailand* 1999, *25*, 113.

44. X. Zou, M. Sundberg, M. Larine and S. Hovmoller, "Structure Projection Retrieval by Image Processing of HTEM Images Taken under Non-Optimum Defocus Conditions," *Ultramicroscopy* 1996, 62, 103-121.
45. Su B.; Lu X.; Lu Q. *Langmuir*, 2008, *24*, 9695-9699.
46. Okamoto A.; Nakamura R.; Osawa H.; Hashimoto K. *Langmuir*, 2008, *24*, 7011-7017.
47. Song S. W.; Hidajat K.; Kawi S.*Langmuir*, 2005, *21*, 9568-9575.
48. Tanglumlert W.; Imae T.; White T.J.; Wongkasemjit S. *J. Am. Ceram. Soc.* 2007, *90*, 3992-3997.

Table 1 Properties of SBA-15 as a function of synthesis route

Synthesis*		Surface Area (m^2/g)	Channel Volume (cm^3/g)	Channel Diameter (Å)			$d_{(10)}/d_{(30)}$
		BET	BET	BET	TEM	SAXS	SAXS
Route 1	Without hydrothermal treatment	486	0.6	50	~45	60-63	3
Route 2	With hydrothermal treatment via microwave assisted method at **100 °C for 2 h.**	572	0.8	55	~45	63-67	2.8
	With hydrothermal treatment via microwave assisted method at **120 °C for 1 h.**	613	0.8	54	~45	63-67	2.8

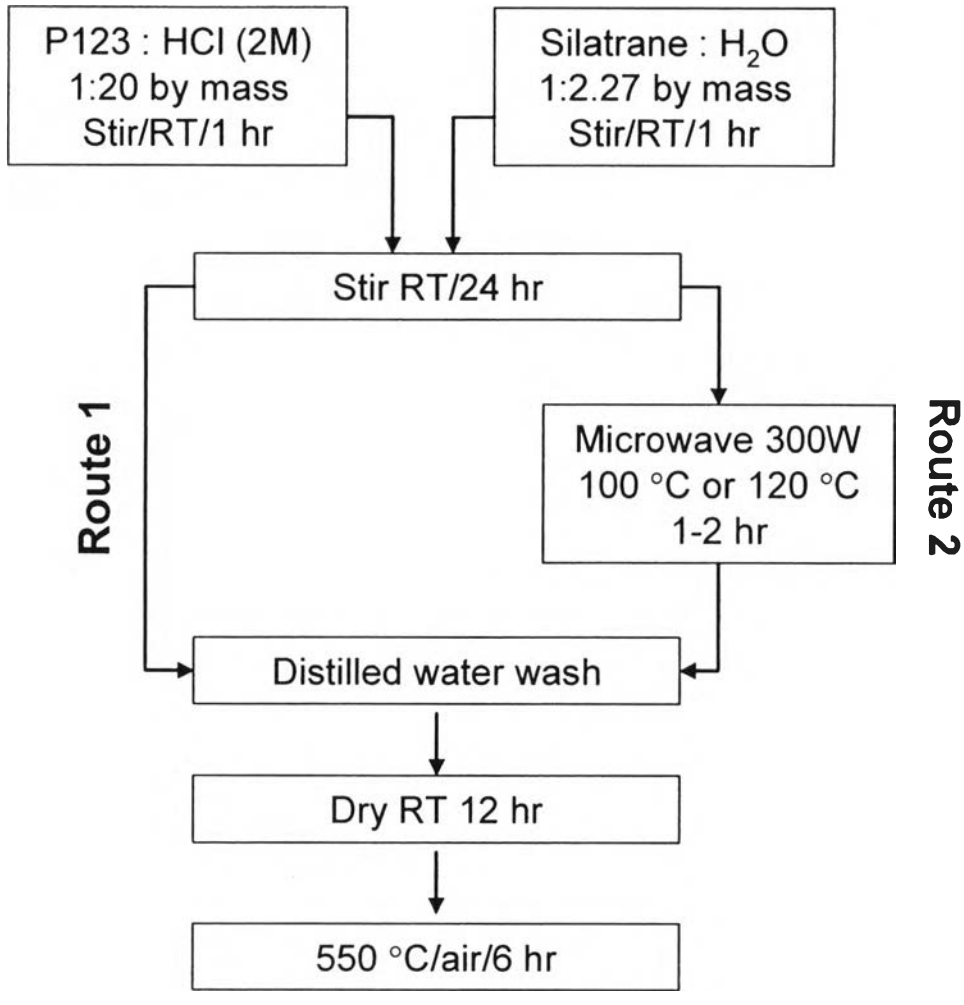

Figure 1 Simplified room temperature synthesis of SBS-15 (Route 1) compared to conventional microwave-assisted hydrothermal method (Route 2).

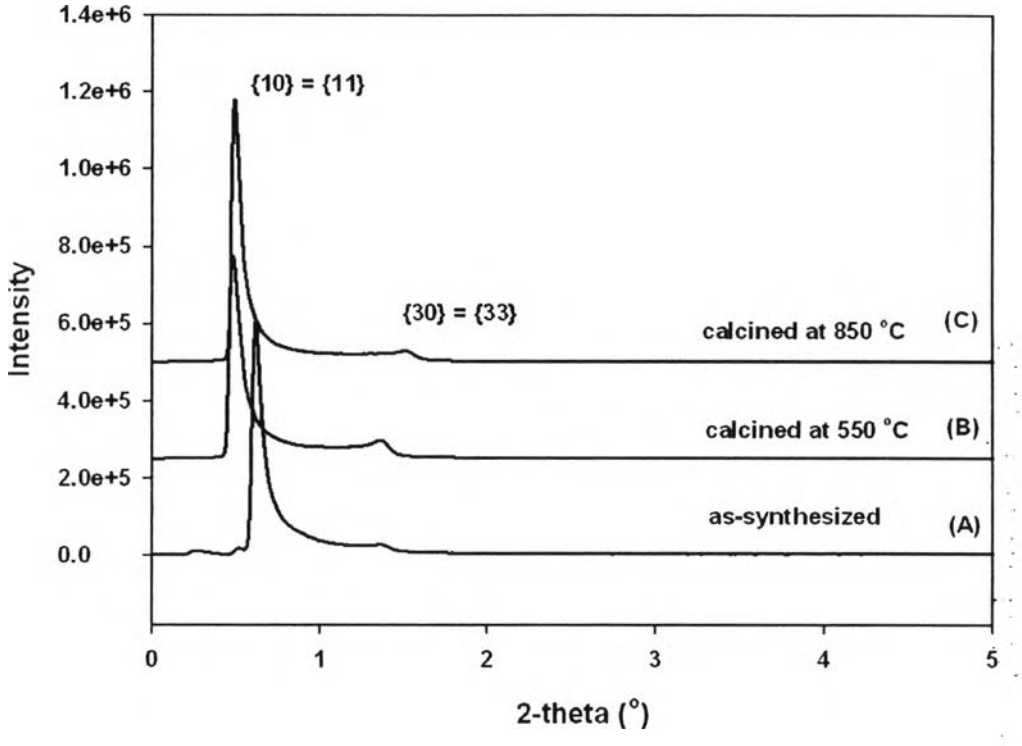

Figure 2 The SAXS pattern of the as-synthesized SBA-15 (A), after calcinations at 550 °C (B) and after calcination at 850 °C (C). These materials show two strong scattering maxima that are indexed in accord with *p6mm* (hexagonal) symmetry.

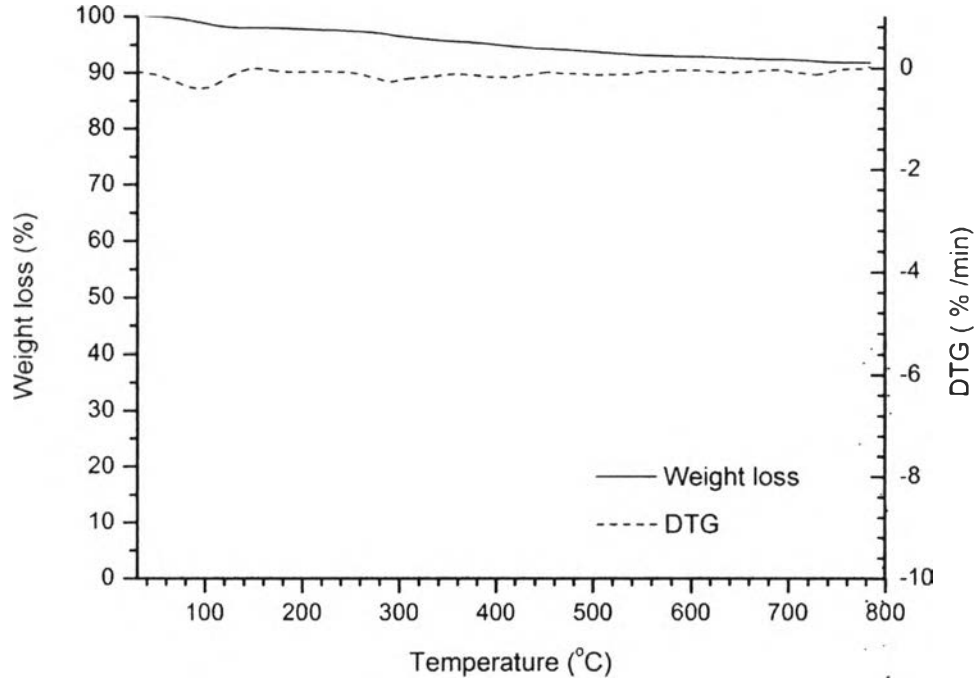

Figure 3 The TG-DTA peak analyzed in air of SBA-15 after calcinations at 550 °C for 6 h.

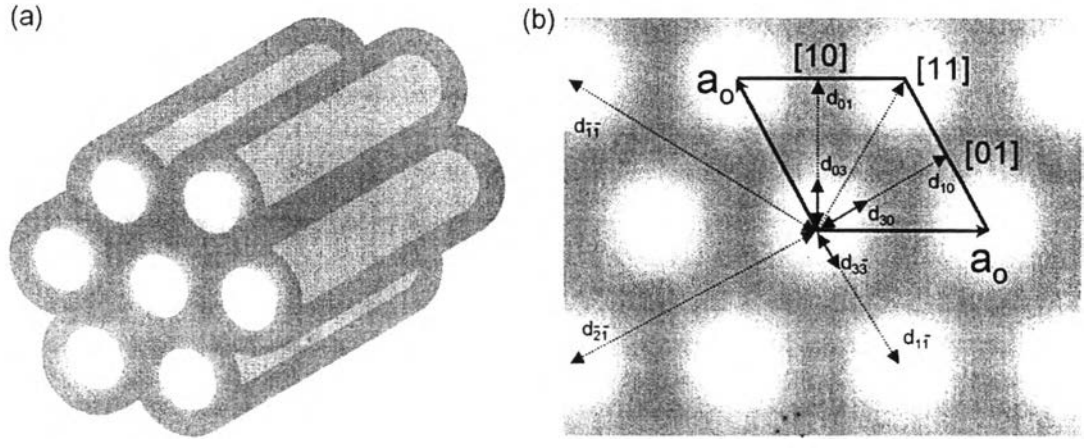

Figure 4 (a) Idealized morphology of the two-dimensional arrangement of silica tubes in SBA-15 and conforming to *p6mm* symmetry. In reality, the tubes are sinuous and extend over a range of diameters which destroys long range hexagonal symmetry. (b) Projection along the mesoporous tubes emphasizing the equivalence of {10} ≡ {11} planes and d-spacings that define the underlying crystallographic repeat, while {30} ≡ {33} correspond to a first approximation to the observed channel diameters.

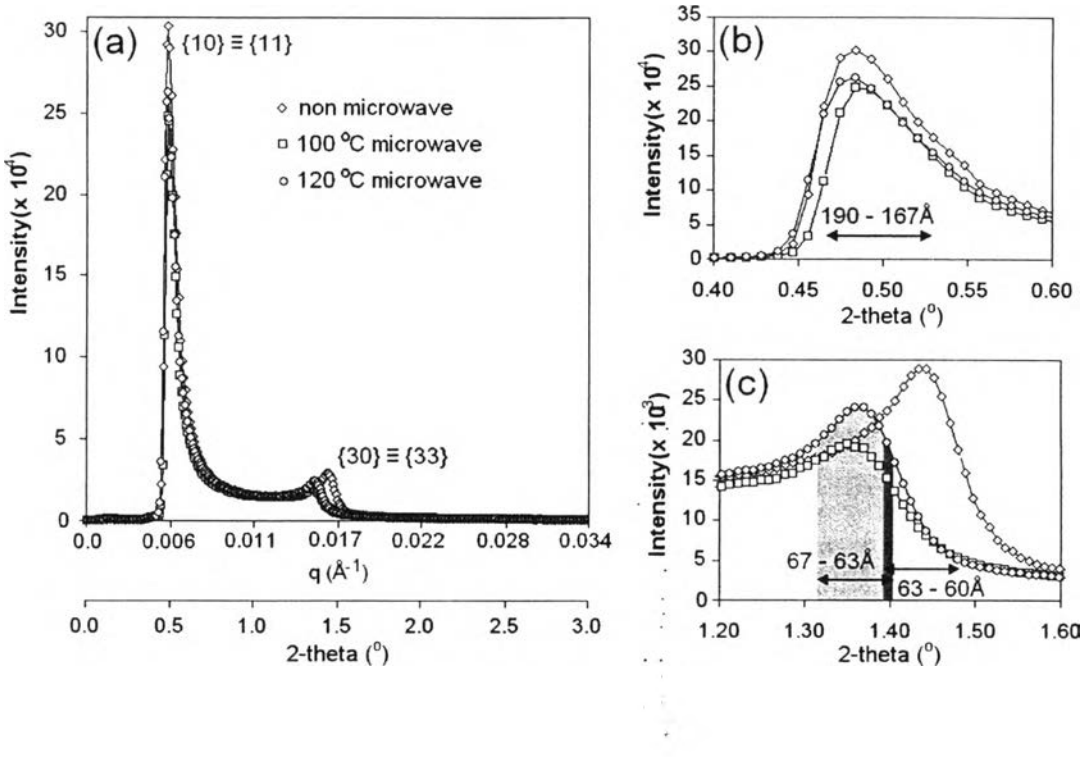

Figure 5 (a) The SAXS pattern the SBA-15 materials show two strong scattering maxima that are indexed in accord with *p6mm* symmetry. The relative positions of these maxima are distinct for those mesoporous structures prepared with the assistance of microwave homogenization. (b) The {10} ≡ {11} reflections are anisotropic and show that the upper limit of the crystallographic repeat in the 2D mesopore order is quite sharp (~190Å) but with a long tail of shorter periodicity down to ~167Å. (c) The {30} ≡ {33} scattering that provides a measure of pore diameter shows the channels are slightly larger when microwave treatment is used, as compared to direct hydrothermal synthesis, in agreement with gas absorption measurements (see Table 1).

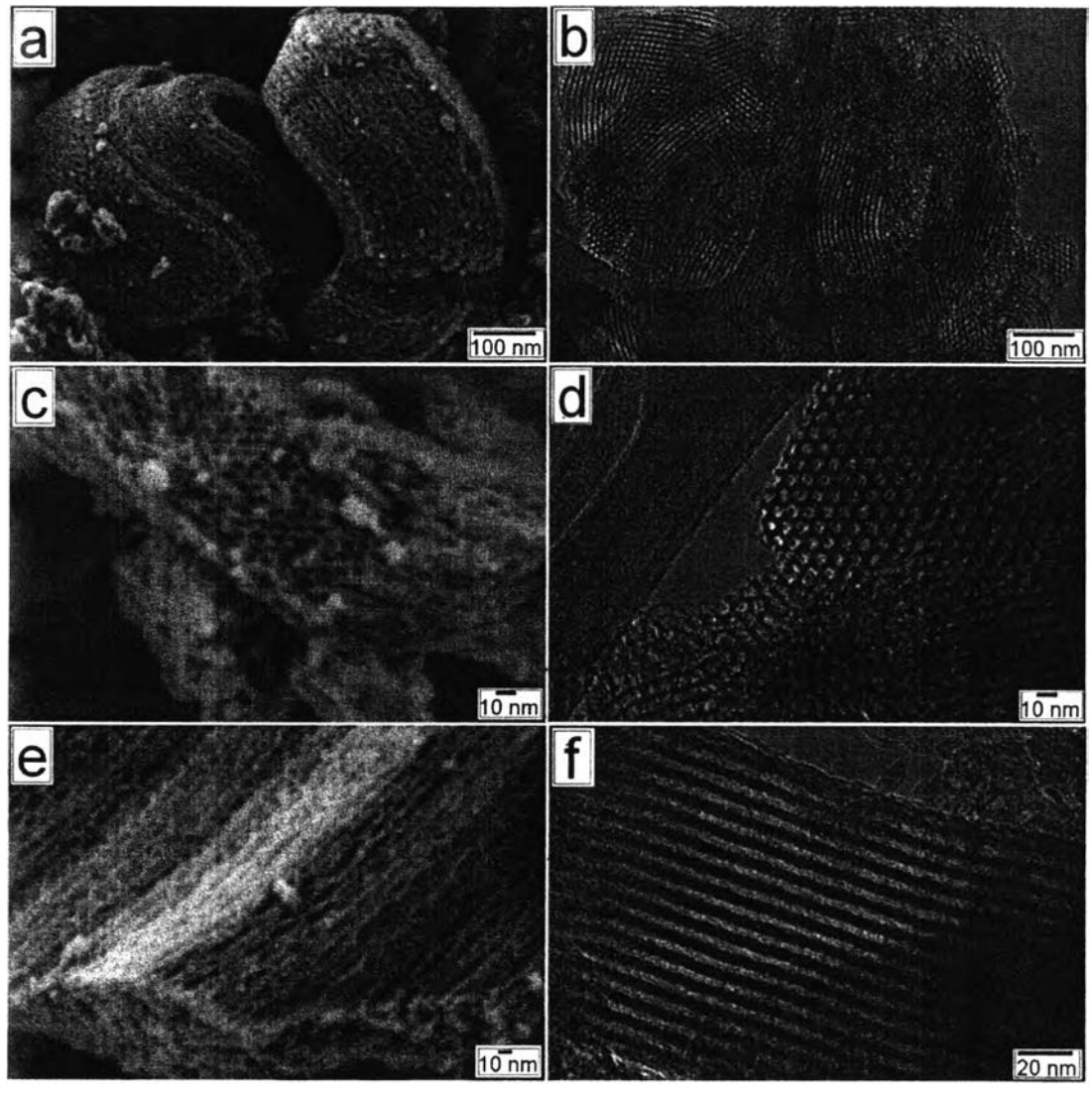

Figure 6 FESEM (left-hand side) and TEM (right-hand side) images of SBA-15 prepared hydrothermally at 120°C/1 h with microwave assistance. (a) & (b) At lower magnifications the twisted bundles of silica tubes are seen to co-exist with less crystalline and aperiodic material. (c) (d) When viewed along the pseudo-hexagonal projection it evident that channels not uniform in shape or content. (e) & (f) In <10> FESEM clearly shows cavitation along the channels. While this is not evident in TEM, the regular periodicity the 2D mesopore order is evident.

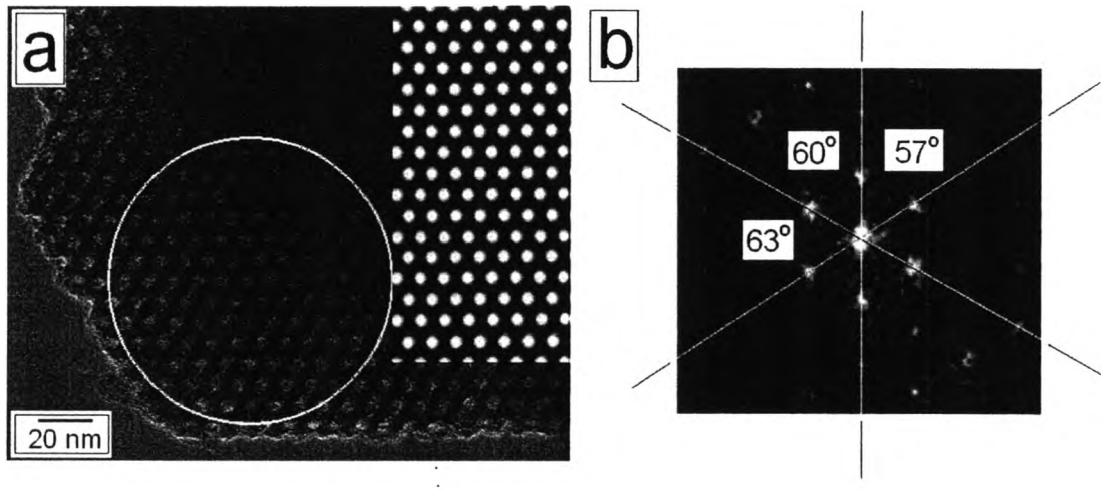

Figure 7 (a) A well-ordered fragment of SBS-15 project in pseudo-*p6mm* projection. (b) The frequency image obtained by fast Fourier transformation (FFT) of the region within the circle yields shows angles that departure from 60° demonstrating that this material fragment better corresponds to *p*2 oblique symmetry. By imposing *p6mm* symmetry and calculating the back Fourier transform the inserted processed image in (a) is generated that yields an average pore diameter of 46 Å.

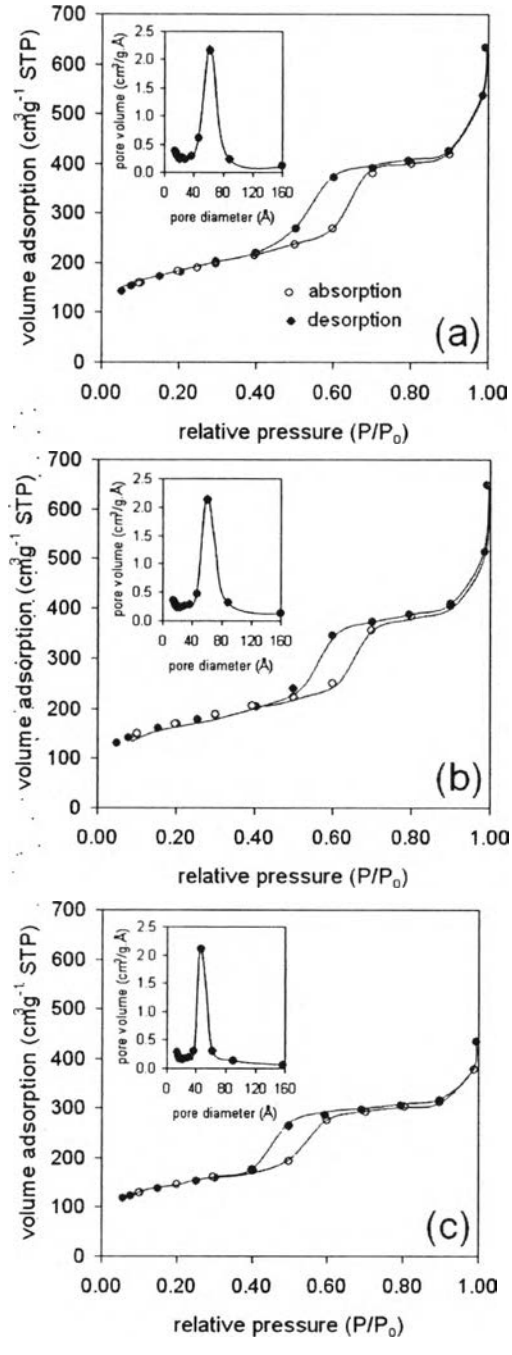

Figure 8 Nitrogen adsorption-desorption isotherms and corresponding pore size distributions for SBA-15 prepared with a microwave-assisted hydrothermal route at (a)120°C /1 h, (b) 100°C /2 h, and (c) directly at RT by stirring. The pore size range is slightly narrower for the latter (FWHM ~ 18 Å) as compared to the former (FWHM ~ 25 Å).

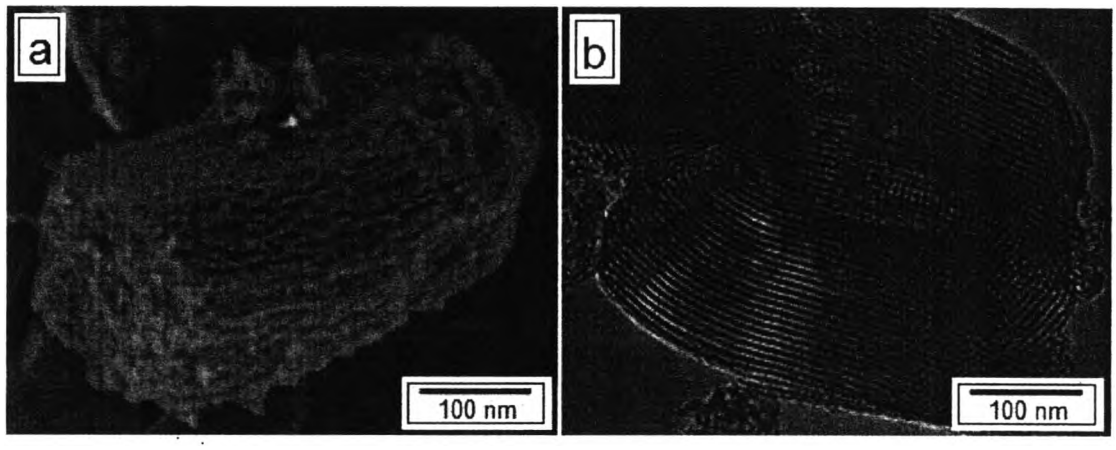

Figure 9 Approximate <10> FESEM (a) and TEM (b) images micrograph of SBA-15 prepared hydrothermally with microwave-assisted method at 100°C/2 h.

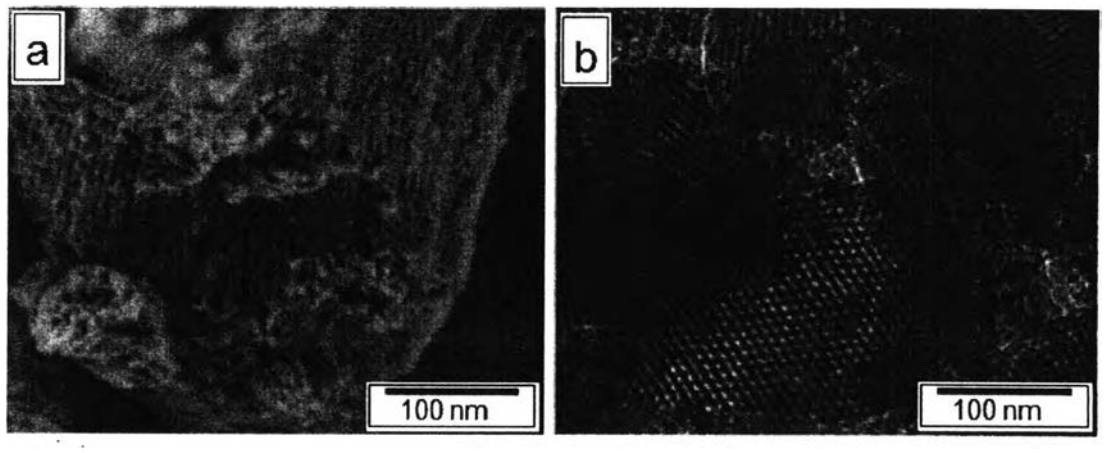

Figure 10 Approximate <10> FESEM (a) and hexagonal TEM (b) images of SBA-15 prepared at RT without hydrothermal treatment.